Photoproduction of C-even quarkonia at the EIC and EicC

Yu Jia,[*] Zhewen Mo,[†] Jichen Pan,[‡] and Jia-Yue Zhang[§]
Institute of High Energy Physics, Chinese Academy of Sciences, Beijing 100049, China
and School of Physics, University of Chinese Academy of Sciences, Beijing 100049, China

(Received 25 August 2022; accepted 22 May 2023; published 25 July 2023)

The η_c photoproduction in ep collision has long been proposed as an ideal process to probe the existence of Odderon. In the current work, we systematically investigate the photoproduction of various C-even heavy quarkonia (exemplified by $\eta_{c(b)}$, and $\chi_{c(b)J}$ with $J = 0, 1, 2$) via one-photon exchange channel, at the lowest order in α_s and heavy quark velocity in the context of Non-relativistic quantum chromodynamics (NRQCD) factorization. We find that the photoproduction rates of η_c through this mechanism are comparable in magnitude with that through the Odderon-initiated mechanism, even in the Regge limit ($s \gg -t$), though the latter types of predictions suffer from considerable theoretical uncertainties. The future measurements of these types of quarkonium photoproduction processes in EIC and EicC are crucial to ascertain which mechanism plays the dominant role.

DOI: 10.1103/PhysRevD.108.016015

I. INTRODUCTION

Recently, the GlueX experiment at JLab reported the first measurement of near-threshold J/ψ photoproduction off the proton [1], which triggered a flurry of theoretical investigations. The central issue is whether one can unambiguously infer the QCD trace anomaly contributions to the proton mass through this "golden" process. The answer is unclear by far and intensive debates are still going on. The projected SoLID experiment [2] is planned to accumulate much higher luminosity for the process $\gamma p \to J/\psi + p$ near threshold. Moreover, future experiments at EIC [3] and EicC [4], designed for the integrated luminosity greater than order 10 fb^{-1}, can measure both J/ψ and Υ photo- and leptoproduction near threshold with better accuracy.

Besides the vector quarkonium near-threshold photoproduction, another type of exclusive quarkonium production processes in ep collision is also of great theoretical interest. Concretely speaking, it has long been proposed that the C-even quarkonium such as η_c photoproduction in the Regge limit (i.e., large s yet small t limit) is an ideal place to look for the existence of the Odderon.

As is well known, long before the advent of QCD, elastic hadron scattering processes in the forward limit have been analyzed in the framework of Regge theory [5], which is built upon some general axiomatic principles of S-matrix theory such as analyticity and unitarity. Two central objects in Regge theory are the Reggeized multigluon compounds responsible for t-channel exchange, with the C-even state called Pomeron [6–10], while the C-odd one called Odderon [11]. In the present work, we concentrate on the effect of Odderon. The C-odd property of Odderon indicates there is a difference between the pp and $p\bar{p}$ elastic scattering in the Regge limit. Apart from early experimental evidence [12–14], a recent careful analysis has been conducted to compare the $p\bar{p}$ elastic cross section measured in the D0 experiment [15] at $\sqrt{s} = 1.96$ TeV, with the pp elastic cross section measured at the LHC experiment [16] extrapolated to $\sqrt{s} = 1.96$ TeV, the 3.4σ level discrepancy [17] is viewed as strong evidence for the existence of the Odderon.

On theoretical ground, Bartels-Kwiecinski-Praszalowicz (BKP) equation [18], an integral equation for the Green functions of three Reggeized gluons in the t-channel plays a central role in the Odderon theory. Two different solutions to the BKP equation are Bartels-Lipatov-Vacca(BLV) Odderon solution [19] and Janik-Wosiek(JW) Odderon solution [20,21], which differ in the quantum number q_3 defined in [21,22] as well as the intercept $\alpha(0)$, characterizing the scaling behavior of the total cross section with s in the Regge limit, $\sigma \sim s^{\alpha(0)-1}$ arising from Regge pole [5]. It appears necessary to examine the different solutions channel by channel.

According to [23,24], both BLV and JW solutions contribute to the $pp/p\bar{p}$ scattering. Consequently,

[*]jiay@ihep.ac.cn
[†]mozw@ihep.ac.cn
[‡]panjichen@ihep.ac.cn
[§]zhangjiayue@ihep.ac.cn

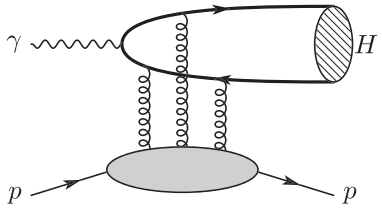

FIG. 1. Three gluon/Odderon t-channel exchange for $\gamma p \to H + p$, where H represents a C-even quarkonium.

concerning only the $pp/p\bar{p}$ forward scattering is not sufficient to single out the correct Odderon model. In contrast, for the C-even neutral meson photoproduction process, the BLV solution yields a nonvanishing contribution, but the JW solution does not contribute because this solution vanishes if two of the three gluons are located at the same spacetime point. Pseudoscalar/tensor neutral meson photo(electro-) production process, such as $f_2(1270)$ [25], π^0 [26,27], $\eta(548)$ [27], *etc.*, is necessary to confirm the BLV solution [23]. Among them, the pseudoscalar charmonium η_c photoproduction has attracted much attention [19,24,28–34]. A representative diagram for the Odderon contribution to $\gamma p \to Hp$ (H representing a C-even quarkonium) is shown in FIG. 1.

It is fair to note that the aforementioned Odderon-based models are subjected to large theoretical uncertainties. Needless to say, it is crucial for the future EIC and EicC experiments to provide the key examination. On the other hand, another important mechanism for the C-even quarkonium photoproduction, i.e., through one-photon t-channel exchange, has not been adequately studied in literature. At least, this one-photon exchange contribution constitutes the important background to pin down the Odderon contribution unambiguously. Moreover, $\gamma p \to Hp$ itself is also of theoretical interest, which provides a novel means to test the applicability of NRQCD effective theory [35] for exclusive quarkonium production in ep collision.

It then becomes the central aim of this work to study the photoproduction of C-even quarkonium $\gamma p \to Hp$ through one-photon exchange, in the framework of NRQCD factorization. The calculation is conducted at the lowest order in α_s and heavy quark velocity expansion. We will consider H to be both S-wave spin-singlet quarkonia $\eta_{c,b}$ and P-wave spin-triplet quarkonia χ_{cJ} (χ_{bJ}) ($J = 0, 1, 2$). Our main finding is that this type of contribution may be comparable in magnitude with the Odderon contribution in the Regge limit, and thus cannot be neglected. We hope the future EIC and EicC experiments can measure these processes and explicitly test our predictions.

The structure of this paper is distributed as follows. In Sec. II, we present the formulas of differential cross sections for the $\gamma p \to Hp$ processes through one-photon exchange mechanism, with $H = \eta_{c,b}, \chi_{cJ}$ (χ_{bJ}) ($J = 0, 1, 2$). The predictions are given by the lowest order calculation within the NRQCD factorization framework. In Sec. III, we discuss the asymptotic behaviors of the differential cross sections in Regge limit and near-threshold limit, respectively. Section IV is devoted to the numerical results and phenomenological analyses. We conclude in Sec. V. For the sake of completeness, yet mainly for amusement, in Appendix we also present the explicit expressions of the differential cross section for $\gamma p \to J/\psi + p$ from the one-graviton t-channel exchange (analogous to one-photon exchange).

II. ONE-PHOTON EXCHANGE MECHANISM FOR QUARKONIUM PHOTOPRODUCTION

Let us turn to the photoproduction process $\gamma p \to Hp$, with H signaling the C-even quarkonium state H exemplifying η_c and χ_{cJ}. The same analysis also applies to bottomonia photoproduction. The leading-order (LO) Feynman diagrams that incorporate the one-photon exchange are depicted in FIG. 2. The amplitude possesses the following factorized structure:

$$\mathcal{M} = \frac{e^2 g_{\mu\nu}}{t} \langle H(P)|J^{\mu}_{\rm EM}|\gamma(k)\rangle \langle p(P_2)|J^{\nu}_{\rm EM}|p(P_1)\rangle, \quad (1)$$

where the external momenta of each particle are specified in the parentheses, the momentum carried by the virtual photon is $q = P - k = P_1 - P_2$, and $t \equiv q^2 \equiv -Q^2$, $s = (P_1 + k)^2 = (P_2 + P)^2$ is the square of enter-of-mass energy. The electromagnetic current $J^{\mu}_{\rm EM}$ bears the standard definition:

$$J^{\mu}_{\rm EM} = \sum_f e_f \bar{q}_f \gamma^{\mu} q_f + \cdots, \quad (2)$$

where we have only retained the quark sector contribution, $e_u = 2/3$ for up-type quark, and $e_d = -1/3$ for down-type quark.

The electromagnetic vertex in the lower half of each Feynman diagram in Fig. 2 encapsulates the contribution from the familiar proton electromagnetic form factors:

$$\langle p(P_2)|J^{\mu}_{\rm EM}|p(P_1)\rangle = \bar{u}(P_2)\left[\gamma^{\mu} F_1(q^2) + \frac{i\sigma^{\mu\nu} q_{\nu}}{2M_p} F_2(q^2)\right] \times u(P_1), \quad (3)$$

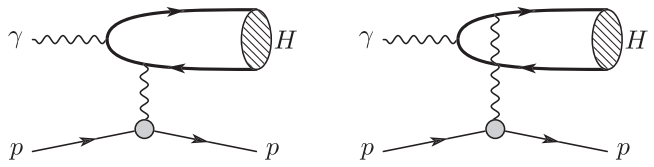

FIG. 2. Two lowest-order Feynman diagrams for C-even quarkonium photoproduction.

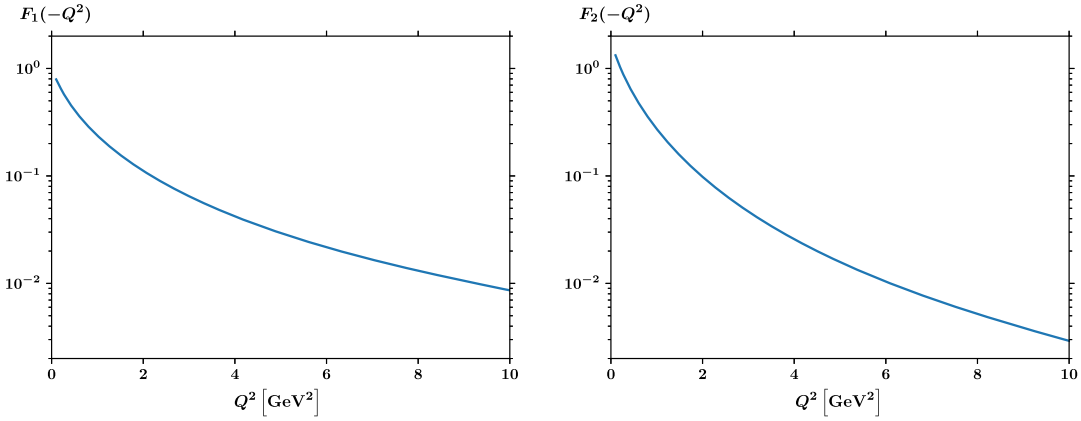

FIG. 3. The experimentally-determined proton electromagnetic form factors F_1 and F_2 as a function of Q^2 [39].

where the form factors $F_1(q^2)$ and $F_2(q^2)$ are real-valued functions. M_p is the mass of proton. The perturbative QCD analysis reveals that the form factors scale asymptotically as $F_1(q^2) \sim 1/q^4$ [36,37], and $F_2(q^2)/F_1(q^2) \sim \log^2(q^2/\Lambda^2)/q^2$ [38]. An explicit plot of the proton form factors versus momentum transfer, obtained through fitting a large set of data [39], is displayed in Fig. 3, which we will use for later numerical analysis.

The $\gamma\gamma^* \to H$ vertex in the upper half of each diagram in Fig. 2 encodes the photon-to-charmonium electromagnetic transition form factor. Irrespective of the explicit value of Q^2, owing to the fact $m_c \gg \Lambda_{\rm QCD}$ and asymptotic freedom, these EM transition form factors can be factorized in the product of the short-distance coefficients and long-distance NRQCD matrix elements. At the lowest order in α_s and heavy quark velocity v, a straightforward calculation leads to the following expressions for various photon-to-H electromagnetic transition form factors, with $H = \eta_c, \chi_{c0,1,2}$:

$$\langle \eta_c(P)|J^\mu_{\rm EM}|\gamma(k)\rangle = -\frac{4ie_c e}{m_c^{1/2}(4m_c^2-t)}\sqrt{\frac{N_c}{2\pi}}R_S(0)\epsilon^{\mu\nu\rho\sigma}\varepsilon_\nu(k)k_\rho P_\sigma, \tag{4a}$$

$$\langle \chi_{c0}(P)|J^\mu_{\rm EM}|\gamma(k)\rangle = \frac{2\sqrt{3}e_c e}{3m_c^{3/2}(4m_c^2-t)^2}\sqrt{\frac{3N_c}{2\pi}}R'_P(0)(12m_c^2-t)[(4m_c^2-t)g^{\mu\nu}-2k^\mu P^\nu]\varepsilon_\nu(k), \tag{4b}$$

$$\begin{aligned}\langle \chi_{c1}(P)|J^\mu_{\rm EM}|\gamma(k)\rangle = &-\frac{\sqrt{2}ie_c e}{m_c^{5/2}(4m_c^2-t)^2}\sqrt{\frac{3N_c}{2\pi}}R'_P(0)\varepsilon^*_\alpha(P)\Big\{2[4m_c^2k^\mu+(t-4m_c^2)P^\mu]\epsilon^{\nu\rho\sigma\alpha}k_\rho P_\sigma - 2tP^\nu\epsilon^{\mu\rho\sigma\alpha}k_\rho P_\sigma \\ &+ t(4m_c^2-t)\epsilon^{\mu\nu\sigma\alpha}P_\sigma\Big\}\varepsilon_\nu(k),\end{aligned} \tag{4c}$$

$$\begin{aligned}\langle \chi_{c2}(P)|J^\mu_{\rm EM}|\gamma(k)\rangle = &\frac{e_c e}{3m_c^{7/2}(4m_c^2-t)^2}\sqrt{\frac{3N_c}{2\pi}}R'_P(0)\varepsilon^*_{\alpha\beta}(P)\Big\{2m_c^2(12m_c^2-t)[(4m_c^2-t)g^{\mu\nu}-2k^\mu P^\nu]g^{\alpha\beta}+96m_c^4g^{\mu\nu}k^\alpha k^\beta \\ &- t[(4m_c^2-t)g^{\mu\nu}-2k^\mu P^\nu]P^\alpha P^\beta - 12m_c^2[(4m_c^2-t)g^{\mu\nu}+(P^\mu-k^\mu)P^\nu](k^\alpha P^\beta+k^\beta P^\alpha) \\ &+ 48m_c^4P^\nu(k^\alpha g^{\beta\mu}+k^\beta g^{\alpha\mu}) - 48m_c^4k^\mu(k^\alpha g^{\beta\nu}+k^\beta g^{\alpha\nu}) + 6m_c^2(4m_c^2-t)(k^\mu+P^\mu)(P^\alpha g^{\beta\nu}+P^\beta g^{\alpha\nu}) \\ &- 24m_c^4(4m_c^2-t)(g^{\alpha\mu}g^{\beta\nu}+g^{\alpha\nu}g^{\beta\mu})\Big\}\varepsilon_\nu(k),\end{aligned} \tag{4d}$$

where $N_c = 3$ is the number of colors, m_c is the mass of charm quark (for the bottomonium case, one simply replaces m_c to m_b, and e_c to e_b), and $\varepsilon_\alpha(P), \varepsilon_{\alpha\beta}(P)$ represent the polarization vector and tensor of χ_{c1}, χ_{c2}, respectively. One readily verifies that the expressions in (4) obey the conservation of the current $J^\mu_{\rm EM}$, Ward identity for the incoming photon, as well as the discrete C, P, T symmetries. In passing, we note that the γ-to-η_c transition form factor has already been computed to $\mathcal{O}(\alpha_s^2)$ [40]. For later phenomenological analysis, it is convenient to

approximate the nonperturbative vacuum-to-H NRQCD matrix elements by the (first derivative of) radial wave functions at the origin $R_S(0)$ [$R'_P(0)$] in potential model.

Starting from the standard formula [41]:

$$\frac{d\sigma(\gamma p \to H + p)}{dt} = \frac{1}{64\pi s}\frac{1}{|\mathbf{k}_{\rm cm}|^2}\frac{1}{2\times 2}\sum_{\rm Polar.}|\mathcal{M}|^2, \tag{5}$$

(with $\mathbf{k}_{\rm cm}$ referring to the magnitude of the photon momentum in the center-of-mass frame), combined with (3) and (4), we then obtain the desired differential rates for photoproduction of H:

$$\begin{aligned}\frac{d\sigma(\gamma p \to \eta_c p)}{dt} = {}& \frac{4\pi e_c^4\alpha^3 N_c|R_S(0)|^2}{m_c t^2(t-4m_c^2)^2(M_p^2-s)^2}\Big\{2[8m_c^2t(M_p^2+s+t)-16m_c^4(2M_p^2+t)-t(2M_p^4-4M_p^2s+2s^2\\ &+2st+t^2)]F_1^2(t)-4t(t-4m_c^2)^2F_1(t)F_2(t)-t\Big[16m_c^4+4m_c^2t\Big(\frac{s}{M_p^2}-3\Big)\\ &+t\Big(-M_p^2+2(s+t)-\frac{s(s+t)}{M_p^2}\Big)\Big]F_2^2(t)\Big\},\end{aligned} \tag{6a}$$

$$\frac{d\sigma(\gamma p \to \chi_{c0} p)}{dt} = \frac{|R'_P(0)|^2}{m_c^2|R_S(0)|^2}\left(\frac{12m_c^2-t}{4m_c^2-t}\right)^2\frac{d\sigma(\gamma p \to \eta_c p)}{dt}, \tag{6b}$$

$$\begin{aligned}\frac{d\sigma(\gamma p \to \chi_{c1} p)}{dt} = {}& \frac{24\pi e_c^4\alpha^3 N_c|R'_P(0)|^2}{m_c^3(t-4m_c^2)^4(M_p^2-s)^2}\Big\{\Big[-t(-4sM_p^2+2M_p^4+2s^2+2st+t^2)+8m_c^2(-M_p^2(4s+t)+2M_p^4\\ &+2s^2+3st+t^2)-16m_c^4(-2M_p^2+4s+t)\Big]F_1^2(t)-4(t-4m_c^2)^2(t+4m_c^2)F_1(t)F_2(t)\\ &+\Big[-2tm_c^2\Big(-2(4s+3t)+4M_p^2+\frac{4s^2+6st+t^2}{M_p^2}\Big)+16tm_c^4\Big(1+\frac{2s+t}{M_p^2}\Big)\\ &-32m_c^6\Big(4+\frac{t}{M_p^2}\Big)-t^2\Big(2(s+t)-M_p^2-\frac{s(s+t)}{M_p^2}\Big)\Big]F_2^2(t)\Big\},\end{aligned} \tag{6c}$$

$$\begin{aligned}\frac{d\sigma(\gamma p \to \chi_{c2} p)}{dt} = {}& \frac{8\pi e_c^4\alpha^3 N_c|R'_P(0)|^2}{m_c^3t^2(t-4m_c^2)^4(M_p^2-s)^2}\Big\{2\Big[8t^2m_c^2(-M_p^2(12s+5t)+6M_p^4+6s^2+7st+t^2)-16tm_c^4(-2M_p^2(12s+5t)\\ &+12M_p^4+12s^2+24st+7t^2)+768tm_c^6(M_p^2+s+t)-1536m_c^8(2M_p^2+t)+t^3(-4sM_p^2+2M_p^4\\ &+2s^2+2st+t^2)\Big]F_1^2(t)-4t(t-4m_c^2)^2(12tm_c^2+96m_c^4+t^2)F_1(t)F_2(t)-t\Big[-16tm_c^4\Big(-(12s+7t)\\ &+6M_p^2+\frac{3(2s^2+4st+t^2)}{M_p^2}\Big)+2t^2m_c^2\Big(-6(4s+t)+12M_p^2+\frac{12s^2+14st+3t^2}{M_p^2}\Big)\\ &-96tm_c^6\Big(8-\frac{4s+t}{M_p^2}\Big)+1536m_c^8+t^3\Big(2(s+t)-M_p^2-\frac{s(s+t)}{M_p^2}\Big)\Big]F_2^2(t)\Big\}.\end{aligned} \tag{6d}$$

The kinematically allowed region for this 2-to-2 process at a given $\sqrt{s}$ is $|t|_{\rm min} \le -t \le |t|_{\rm max}$, with

$$|t|_{\rm min} = -\frac{M_H^2(s+M_p^2)-(s-M_p^2)\Big(s-M_p^2-\sqrt{\lambda(s,M_p^2,M_H^2)}\Big)}{2s}, \tag{7a}$$

$$|t|_{\rm max} = -\frac{M_H^2(s+M_p^2)-(s-M_p^2)\Big(s-M_p^2+\sqrt{\lambda(s,M_p^2,M_H^2)}\Big)}{2s}. \tag{7b}$$

M_H denotes the mass of hadron, and $\lambda(x,y,z) = x^2 + y^2 + z^2 - 2xy - 2yz - 2zx$ is the Källen function. One may see [42] for a more detailed discussion.

III. ASYMPTOTIC BEHAVIOR

A. Regge limit

In this work we are primarily interested in the Regge limit. If we presume this limit is set by $s \gg (2m_c)^2 \gg |t|$, one then anticipates that the differential rate near $|t|_{\min} \to M_p^2(2m_c)^4/s^2$ [obtained from the explicit definition of (7)] is the desired asymptotic behavior. However, by closely inspecting the actual numerical results shown in Fig. 4(c) and Fig. 5(b), one sees that the differential production rates fall off rather stiffly as $t \to -|t|_{\min}$. Therefore, $d\sigma/dt$ at $t = -|t|_{\min}$ is not representative for the small $|t|$ behavior that one is really interested in. The asymptotic expressions below are actually derived in the region where $s \gg (2m_c)^2$ and $|t|_{\min} \ll |t| \ll M_p^2 < (2m_c)^2$[1]:

$$\frac{d\sigma(\gamma p \to \eta_c p)}{dt} \approx \frac{\pi e_c^4 \alpha^3 N_c |R_S(0)|^2 F_1^2(0)}{m_c^5(-t)}, \tag{8a}$$

$$\frac{d\sigma(\gamma p \to \chi_{c0} p)}{dt} \approx \frac{9\pi e_c^4 \alpha^3 N_c |R'_P(0)|^2 F_1^2(0)}{m_c^7(-t)}, \tag{8b}$$

$$\frac{d\sigma(\gamma p \to \chi_{c1} p)}{dt} \approx \frac{3\pi e_c^4 \alpha^3 N_c |R'_P(0)|^2 F_1^2(0)}{m_c^9}, \tag{8c}$$

$$\frac{d\sigma(\gamma p \to \chi_{c2} p)}{dt} \approx \frac{12\pi e_c^4 \alpha^3 N_c |R'_P(0)|^2 F_1^2(0)}{m_c^7(-t)}. \tag{8d}$$

From (8) one immediately observes that the differential photoproduction rates are independent of s in the Regge limit. An interesting pattern is that, in the small $|t|$ limit, the η_c, χ_{c0} and χ_{c2} photoproduction rates scale as $\mathcal{O}(1/t)$, whereas the χ_{c1} differential rate exhibits quite differential scaling $\propto t^0$. These scaling behaviors can also be clearly visualized in Fig. 4(c) and Fig. 5(b), which can be ascribed to the Landau-Yang theorem. It should also be emphasized that, though (8) are insensitive to s when $\sqrt{s}$ increases, the lower limit of $|t|$ where (8) remains applicable continues to decrease toward $|t|_{\min}$. As a result, for the total cross section of $\eta_{c(b)}$, $\chi_{c(b)0}$ and $\chi_{c(b)2}$, the t-integrals of (8) yield a $\log s$ enhancement, while the total cross sections for $\chi_{c(b)1}$ photoproduction remains constant in the large s limit, which can be seen from Figs. 7(a) and 7(b).

B. Threshold limit

It is also interesting to consider another very different limit, $\sqrt{s} \approx M_H + M_p$, where the center-of-mass energy is just enough to produce the static H and p in the final state. In such as limit, t can be fixed to be $t_0 = -4M_p m_c^2/(M_p + 2m_c)$. In the near-threshold limit, various differential photoproduction rates can be approximated as

$$\frac{d\sigma(\gamma p \to \eta_c p)}{dt} \approx \frac{\pi e_c^4 \alpha^3 N_c |R_S(0)|^2 (F_1(t_0) + F_2(t_0))^2 (M_p + 2m_c)}{8M_p m_c^5 (M_p + m_c)^2}, \tag{9a}$$

$$\frac{d\sigma(\gamma p \to \chi_{c0} p)}{dt} \approx \frac{\pi e_c^4 \alpha^3 N_c |R'_P(0)|^2 (F_1(t_0) + F_2(t_0))^2 (M_p + 2m_c)(2M_p + 3m_c)^2}{8M_p m_c^7 (M_p + m_c)^4} \tag{9b}$$

$$\begin{aligned}\frac{d\sigma(\gamma p \to \chi_{c1} p)}{dt} \approx{}& \frac{3\pi e_c^4 \alpha^3 N_c |R'_P(0)|^2 (M_p + 2m_c)}{16M_p m_c^9 (M_p + m_c)^4} (F_1^2(t_0) M_p^2 (M_p^2 + 4M_p m_c + 5m_c^2) \\ & -4F_1(t_0)F_2(t_0) M_p m_c^3 + F_2^2(t_0) m_c^2 (M_p^2 + m_c^2)),\end{aligned} \tag{9c}$$

$$\begin{aligned}\frac{d\sigma(\gamma p \to \chi_{c2} p)}{dt} \approx{}& \frac{\pi e_c^4 \alpha^3 N_c |R'_P(0)|^2 (M_p + 2m_c)}{16M_p m_c^9 (M_p + m_c)^4} (F_1^2(t_0)(3M_p^4 + 12M_p^3 m_c + 19M_p^2 m_c^2 + 24M_p m_c^3 + 24m_c^4) \\ & + 4F_1(t_0)F_2(t_0) m_c^2 (2M_p^2 + 9M_p m_c + 12m_c^2) + F_2^2(t_0) m_c^2 (7M_p^2 + 24M_p m_c + 27m_c^2)).\end{aligned} \tag{9d}$$

As it should be, the angular distributions of the H are always isotropic in the near-threshold limit, and the integrated cross sections are suppressed by the relative velocity between the H and proton P, $\propto \sqrt{s - (M_p + M_H)^2}$.

[1]We found that, in the $s \gg (2m_c)^2$ and small $|t|$ limit, our result of $d\sigma(\gamma p \to \eta_c p)/dt$ differs from [43] where a straightforward $t = -|t|_{\min}$ limit is taken.

IV. NUMERICAL ANALYSIS

A. Photoproduction rates

To make explicit phenomenological predictions, we first need to fix the values of various input parameters. We choose the values of the charmonium (bottomonium) wave function at origin from the Cornell potential model [44].

$$M_p = 0.938\ \text{GeV}, \qquad m_c = 1.5\ \text{GeV}, \qquad m_b = 4.7\ \text{GeV}. \tag{10a}$$

$$|R_{1S(c\bar{c})}|^2 = 1.0952\ \text{GeV}^3, \quad |R'_{1P(c\bar{c})}(0)|^2 = 0.1296\ \text{GeV}^5, \tag{10b}$$

$$|R_{1S(b\bar{b})}|^2 = 5.8588\ \text{GeV}^3, \quad |R'_{1P(b\bar{b})}(0)|^2 = 1.6057\ \text{GeV}^5. \tag{10c}$$

In Fig. 4 and Fig. 5 we show the profiles differential photoproduction rates of C-even charmonia and bottomonia at several benchmark points of center-of-mass energy. Typically, we choose $\sqrt{s} = 4.3$ GeV (near charmonium threshold), 15 GeV (near bottomium threshold), and 50 GeV (high energy limit).

Remarkably, in Fig. 6 we also make a detailed comparative study between the one-photon exchange prediction and the Odderon model predictions [24,28] for η_c photoproduction. We take the center-of-mass energy $\sqrt{s} = 15$, 50 GeV. Curiously, one finds that in the low-$|t|$ region, the one-photon exchange contribution is comparable with in magnitude, or even larger than, the Odderon exchange contributions. This implies that it is mandatory to include the one-photon exchange contribution in confrontation from future experimental measurements, even though the ultimate goal is to probe the Odderon contribution in an unambiguous way.

The integrated photoproduction cross sections as a function of $\sqrt{s}$ are displayed in Fig. 7. One can see that the total cross sections for η_c and $\chi_{c0,2}$ photoproduction are of order 10^2 pb in large $\sqrt{s}$, whereas the cross sections

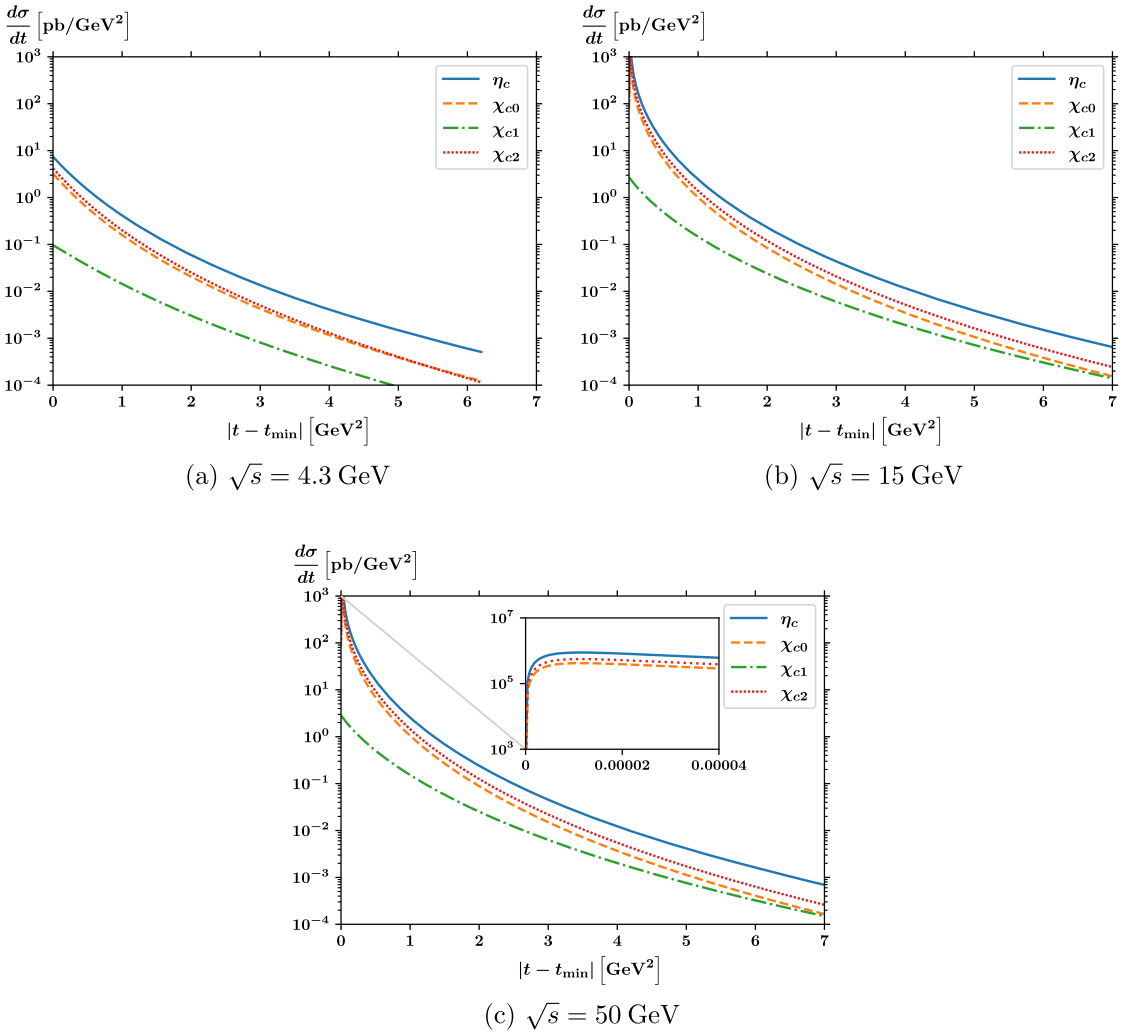

(a) $\sqrt{s} = 4.3$ GeV (b) $\sqrt{s} = 15$ GeV

(c) $\sqrt{s} = 50$ GeV

FIG. 4. The differential production rates for C-even charmonia at different center-of-mass energy, (a), (b), (c).

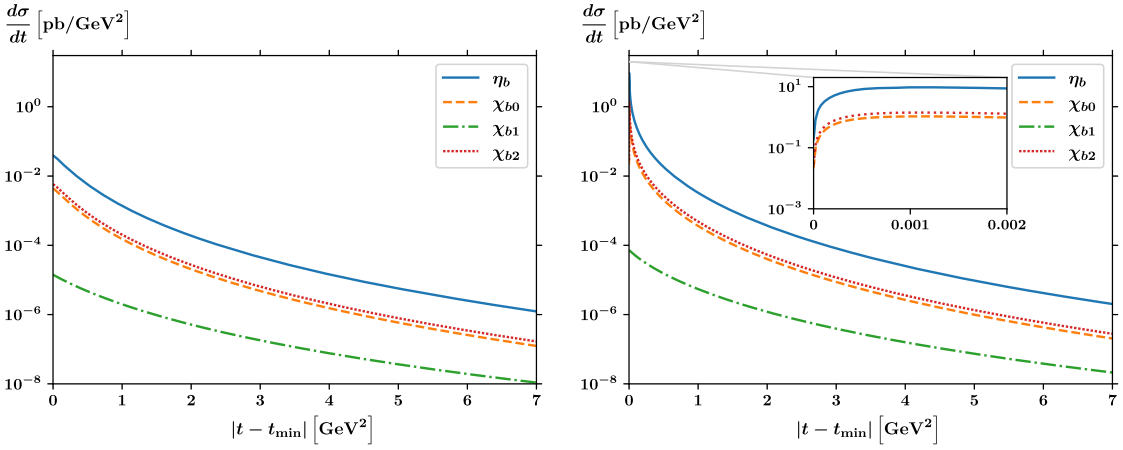

(a) $\sqrt{s} = 15$ GeV (b) $\sqrt{s} = 50$ GeV

FIG. 5. The differential production rates for C-even bottomonia at different $\sqrt{s}$, (a), (b).

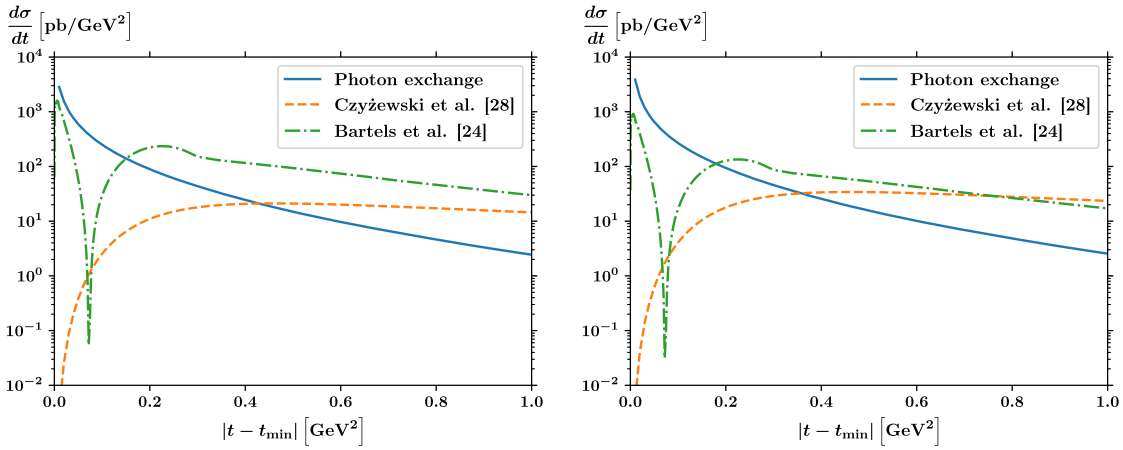

(a) $\sqrt{s} = 15$ GeV (b) $\sqrt{s} = 50$ GeV

FIG. 6. The differential photoproduction rates of η_c at different $\sqrt{s}$ via the one-photon exchange mechanism, compared with the prediction from two Odderon exchange models [24,28].

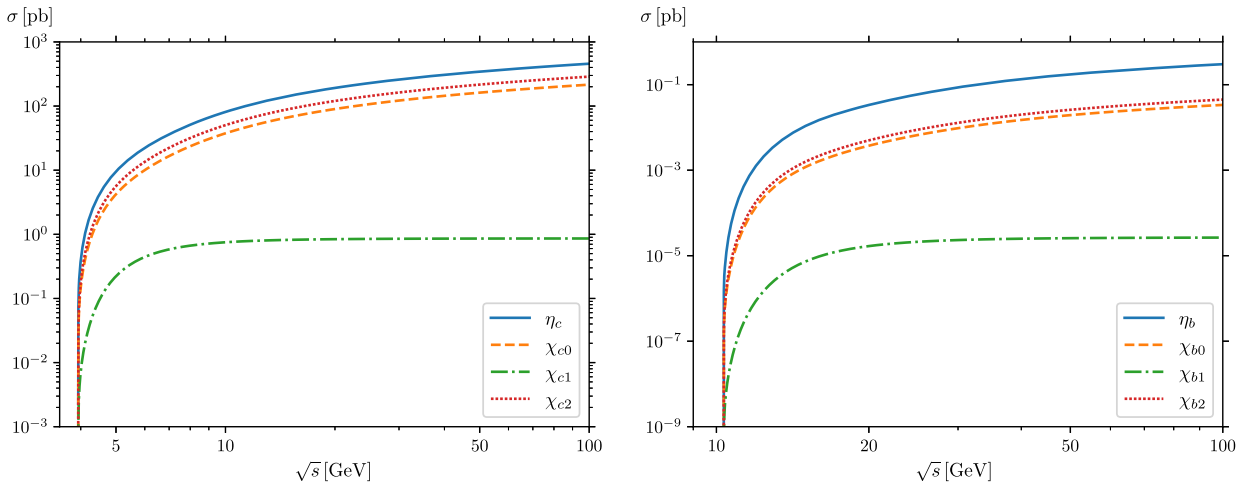

(a) charmonia (b) bottomonia

FIG. 7. The integrated photoproduction rates for C-even charmonia (a) and bottomonia (b).

for η_b and $\chi_{b0,2}$ are much smaller, roughly of order 10^{-2}–10^{-1} pb. Compared with the $\chi_{c(b)0,2}$ channels, the cross sections for $\chi_{c(b)1}$ photoproduction are much suppressed at high energy. This phenomenon can be explained as follows. Clearly the main contribution to the total photoproduction cross section comes from the low-$|t|$ region, where the exchanged photon becomes quasi-real. In such a limit, one can utilize the equivalent photon approximation (EPA). The metric tensor in the numerator of the photon propagator (Fig. 2) can be reexpressed in terms of four photon polarization vectors

$$-g^{\mu\nu} = -\varepsilon_+^{\mu}(q)\varepsilon_-^{\nu*}(q) - \varepsilon_-^{\mu}(q)\varepsilon_+^{\nu*}(q) + \sum_i \varepsilon_{Ti}^{\mu}(q)\varepsilon_{Ti}^{\nu*}(q). \tag{11}$$

$\varepsilon_{Ti}^{\mu}(q)$ are transverse polarization vectors, defined in a frame where $\varepsilon_+^{\mu}(q) = \frac{1}{\sqrt{2}}(1,0,0,1)^T \propto q^{\mu}$ and $\varepsilon_-^{\mu}(q) = \frac{1}{\sqrt{2}}(1,0,0,-1)^T$. The contraction between $\varepsilon_+^{\mu(*)}(q)$ with $\langle H|(J_{\rm EM})_{\mu}|\gamma\rangle$ or $\langle p'|(J_{\rm EM})_{\mu}|p\rangle$ in (1) yields vanishing contributions by the Ward identity. The contraction between $\varepsilon_{Ti}^{\mu}(q)$ with $\langle\chi_{c(b)1}|(J_{\rm EM})_{\mu}|\gamma\rangle$ also gives zero in the $t \to 0$ limit, since $\chi_{c1} \to \gamma\gamma$ is forbidden by the Landau-Yang theorem. Therefore the amplitude for χ_{c1} photoproduction is severely suppressed in the small $|t|$ limit. A direct calculation shows this suppression gives rise to an overall t factor that cancels the denominator in (1). The explicit scaling behavior with t for quarkonium photoproduction can also be seen from the denominators of differential cross sections in (8).

B. Equivalent photon approximation

In order to estimate the quarkonium photoproduction rates in realistic ep collision experiments such as EIC and EicC, one often invokes the equivalent photon approximation [45–47] to assume the photon emitted off the incident electron carrying small virtuality Q'^2. The exclusive quarkonium production rate in ep collision can be factorized as [47]

$$\sigma(ep \to eHp) \approx \int_{k_{\rm min}}^{E_e} dk \int_{Q'^2_{\rm min}}^{Q'^2_{\rm max}} dQ'^2 \frac{d^2N_\gamma}{dkdQ'^2}\sigma(\gamma p \to Hp), \tag{12}$$

with the photon flux defined as

$$\frac{d^2N_\gamma}{dkdQ'^2} = \frac{\alpha}{\pi k Q'^2}\left[1 - \frac{k}{E_e} + \frac{k^2}{2E_e^2} - \left(1 - \frac{k}{E_e}\right)\frac{Q'^2_{\rm min}}{Q'^2}\right], \tag{13}$$

where k and E_e are the photon and electron energies in the target rest frame. $k_{\rm min} = E_e M_H(M_H + 2M_p)/(s_{ep} - M_p^2)$, $Q'^2_{\rm min} = m_e^2 k^2/(E_e(E_e - k))$. We choose $Q'^2_{\rm max} = 0.01$ GeV^2 to be the criterion for identifying a photoproduction event.[2] We take the $\chi_{c(b)0}$ photoproduction rates as a reference basis for the estimation. The cross sections for $\chi_{c(b)2}$ are roughly equal to that for $\chi_{c(b)0}$, while the cross section for η_c is roughly twice that of χ_{c0}, but the cross section of η_b is roughly 10 times larger than that of χ_{b0}.

After carrying out the numerical integration in (12) at $\sqrt{s_{ep}} = 50$ GeV, the typical center-of-mass energy at EIC, the photoproduction rates in ep collision can reach 7.5 pb for χ_{c0} and 0.35 fb for χ_{b0}. Concerning the projected high integrated luminosity of 50 fb^{-1}/year at EicC [4] and 1.5 fb^{-1}/month at EIC [3], these C-even quarkonia photoproduction processes have a bright prospect to be observed in the future EicC and EIC experiments.

For comparison, we also estimate photoproduction rate η_c in the near-threshold limit. We assume $\sqrt{s} = 4.6$ GeV, which corresponds to $E_\gamma \approx 11$ GeV in the proton rest frame, which lies within the energy range of the GlueX experiment($\sqrt{s} < 6$ GeV, with $E_\gamma < 15$ GeV [1]). The η_c production rate is estimated to be about 5 pb. Since the integrated luminosity of the GlueX experiment is only about 68 pb^{-1} [1], and the reconstruction efficiency for η_c and χ_{cJ} is much lower than J/ψ, it is difficult to observe these photoproduction processes of C-even charmonia in the current JLab facilities.

V. CONCLUSION

In the present paper, we analyze the photoproduction of C-even quarkonia via the one-photon exchange mechanism. The main result is that even in the Regge limit, the photoproduction rates for most channels through this mechanism are comparable to or even greater than the predictions based on Odderon exchange models [24,28]. They have bright prospects to be observed in future EIC and EicC experiments. As an interesting exception, the photoproduction rates for $\chi_{c/b,1}$ are much suppressed relative to other channels in the Regge limit, as a consequence of Landau-Yang theorem. Due to the lacking of one-photon exchange contribution, perhaps the future observation of the $\chi_{c/b,1}$ photoproduction events may be viewed as strong evidence for the Odderon exchange model.

ACKNOWLEDGMENTS

This work is supported in part by the National Natural Science Foundation of China under Grants No. 11925506, No. 12070131001 (CRC110 by DFG and NSFC).

[2] According to [3], choosing $Q^2_{\rm max}$ to be 0.01 or 0.1 does not affect the order of magnitude of the estimated cross section.

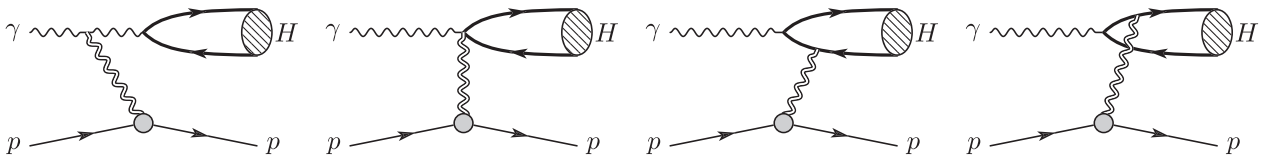

FIG. 8. Feynman diagrams in the LO gravitational contribution.

APPENDIX: ONE-GRAVITON EXCHANGE FOR J/ψ PHOTOPRODUCTION

Understanding the origin of proton mass from QCD has been a fascinating topic for years. The QCD trace anomaly is believed to make important contribution to the proton mass. It has been proposed that J/ψ photoproduction near threshold could be a golden channel to infer the QCD trace anomaly contribution to the proton mass [48]. However, it has also been criticized that some phenomenological assumptions such as vector meson dominance have been adopted in [48].

A closely related topic is the gravitational form factor (GFF) of the proton, from which one can deduce the mass and stress/pressure distributions of the proton. It is rather difficult to extract the proton GFF directly from the scattering experiment. So far the best knowledge about the proton GFF is from lattice QCD simulation [49,50].

In this appendix, analogous to $\gamma p \to \eta_c p$ process via the one-photon exchange, we calculate the photoproduction process $\gamma p \to J/\psi p$ through one-graviton exchange. The corresponding LO Feynman diagrams are shown in shown in Fig. 8. It is certainly hopeless to observe this graviton-induced process in any terrestrial collision experiments, we include the corresponding results mainly for amusement. Note that unlike the photon which is C-odd, the graviton is C-even, therefore the final quarkonium has to be the C-odd state such as J/ψ.

The corresponding photoproduction amplitude can be written in a product of matrix elements of the symmetric (Belinfante) energy-momentum tensor $\Theta_{\mu\nu}$:

$$i\mathcal{M} = \langle J/\psi(P)|\Theta_{\mu\nu}|\gamma(k)\rangle \frac{-i\mathcal{P}^{\mu\nu\rho\sigma}}{q^2}\langle p(P_2)|\Theta_{\rho\sigma}|p(P_1)\rangle, \tag{A1}$$

with $\mathcal{P}^{\mu\nu\rho\sigma} = \frac{1}{2}(g^{\mu\rho}g^{\nu\sigma} + g^{\mu\sigma}g^{\nu\rho} - g^{\mu\nu}g^{\rho\sigma})$. The corresponding matrix element of $\Theta_{\mu\nu}$ for proton is nothing but the proton GFF, which is often parametrized as

$$\langle p(P_2)|\Theta_{\mu\nu}|p(P_1)\rangle = \kappa\bar{u}(P_2)\left[A(t)\frac{P_\mu P_\nu}{M_p} + B(t)\frac{iP_{\{\mu}\sigma_{\nu\}\rho}\Delta^\rho}{2M_p} + D(t)\frac{\Delta_\mu\Delta_\nu - \eta_{\mu\nu}\Delta^2}{4M_p}\right]u(P_1), \tag{A2}$$

$$P = \frac{1}{2}(P_1 + P_2), \qquad \Delta = P_2 - P_1, \qquad t = \Delta^2, \tag{A3}$$

where the Lorentz scalars A, B, D are functions of the momentum transfer.

The γ-to-J/ψ gravitational transition form factor can also be computed in NRQCD factorization. At the lowest order in α_s and v, it reads

$$\Theta^{\mu\nu} = \bar{\psi}\gamma^{(\mu}i\overleftrightarrow{D}^{\nu)}\psi + \frac{1}{4}g^{\mu\nu}F^2 - F^{\mu\rho}F^\nu_\rho, \tag{A4}$$

$$\begin{aligned}\langle J/\psi(P)|\Theta^{\mu\nu}|\gamma(k)\rangle = {}& \frac{1}{6m_c^{3/2}(k\cdot P)}\sqrt{\frac{N_c}{2\pi}}R_S(0)\varepsilon^*_\sigma(P)\varepsilon_\rho(k)e\kappa(g^{\mu\nu}g^{\rho\sigma}(k\cdot P)^2 - g^{\mu\rho}g^{\nu\sigma}(k\cdot P)^2 - k^\sigma P^\rho g^{\mu\nu}(k\cdot P) + k^\sigma P^\nu g^{\mu\rho}(k\cdot P)\\
&+ k^\sigma P^\mu g^{\nu\rho}(k\cdot P) + g^{\mu\sigma}(2m_c^2 - k\cdot P)(g^{\nu\rho}(k\cdot P) - k^\nu P^\rho) - k^\nu P^\mu g^{\rho\sigma}(k\cdot P) - 2m_c^2 k^\nu k^\sigma g^{\mu\rho}\\
&+ k^\mu(-2m_c^2 k^\sigma g^{\nu\rho} + 4m_c^2 k^\nu g^{\rho\sigma} + P^\rho g^{\nu\sigma}(k\cdot P - 2m_c^2) - P^\nu g^{\rho\sigma}(k\cdot P)) + 2m_c^2 g^{\mu\rho}g^{\nu\sigma}(k\cdot P)),\\
k\cdot P = {}& 2m_c^2 - \frac{t}{2},\end{aligned} \tag{A5}$$

where k is the incoming momentum of the photon and P is the momentum of the outgoing J/ψ. One can readily verify that the above expressions obey Ward identity and the conservation of $\Theta_{\mu\nu}$.

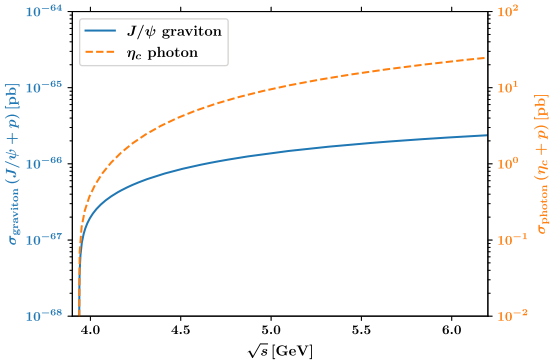

FIG. 9. Comparison of the photoproduction rates between photon induced η_c production and graviton-induced J/ψ production.

After some straightforward calculation, the differential photoproduction rate of J/ψ via graviton exchange reads

$$\begin{aligned}\frac{d\sigma}{dt}_{\text{graviton}} &= \frac{e^2\kappa^4 N_c |R_S(0)|^2}{288\pi M_p^2 m_c^3 (t-4m_c^2)^2}\Bigg(A^2(t)(4M_p^2-t)\Big(M_p^4-2M_p^2 s+t(s-m_c^2)+(s-2m_c^2)^2\Big)^2 \\ &+ 2A(t)\Bigg(D(t)m_c^4(4M_p^2-t)(-2M_p^2-4m_c^2+2s+t)^2+2B(t)t\Big(M_p^4-2M_p^2 s+t(s-m_c^2)+(s-2m_c^2)^2\Big)^2\Bigg) \\ &+ D^2(t)m_c^4(4M_p^2-t)(t-4m_c^2)^2+4D(t)B(t)m_c^4 t(-2M_p^2-4m_c^2+2s+t)^2-4B^2(t)\Bigg(M_p^8 t+2M_p^6 \\ &\times(8m_c^4+m_c^2 t-t(2s+t))+2M_p^4(16m_c^6-8m_c^4(2s+t)+m_c^2 t(t-6s)+3st(s+t)) \\ &+ M_p^2(64m_c^8-16m_c^6(4s+t)+4m_c^4(4s^2-2st-t^2)+m_c^2 t(18s^2+14st+t^2)-2st(s+t)(2s+t)) \\ &+ t\Big(t(s-m_c^2)+(s-2m_c^2)^2\Big)^2\Bigg)\Bigg) \end{aligned} \tag{A6}$$

where $\kappa^2 = 32\pi G_N = 6.75\times 10^{-37}$ GeV^{-2}. Adopting the lattice QCD estimates of the proton GFF [49,50], we find that the integrated cross section for $\gamma p \to J/\psi p$ is about 66 orders of magnitude smaller than that $\gamma p \to \eta_c p$ via one-photon exchange (See Fig. 9).

[1] A. Ali *et al.* (GlueX Collaboration), Phys. Rev. Lett. **123**, 072001 (2019).
[2] J. P. Chen *et al.* (SoLID Collaboration), arXiv:1409.7741.
[3] R. Abdul Khalek, A. Accardi, J. Adam, D. Adamiak, W. Akers, M. Albaladejo, A. Al-bataineh, M. G. Alexeev, F. Ameli, P. Antonioli *et al.*, Nucl. Phys. **A1026**, 122447 (2022).
[4] D. P. Anderle, V. Bertone, X. Cao, L. Chang, N. Chang, G. Chen, X. Chen, Z. Chen, Z. Cui, L. Dai *et al.*, Front. Phys. (Beijing) **16**, 64701 (2021).
[5] C. Ewerz, arXiv:hep-ph/0306137.
[6] A. Donnachie and P. V. Landshoff, Phys. Lett. B **470**, 243 (1999).
[7] J. M. Laget and R. Mendez-Galain, Nucl. Phys. **A581**, 397 (1995).
[8] A. Donnachie and P. V. Landshoff, Phys. Lett. B **348**, 213 (1995).
[9] A. Donnachie and P. V. Landshoff, Nucl. Phys. **B311**, 509 (1989).
[10] A. Sibirtsev, S. Krewald, and A. W. Thomas, J. Phys. G **30**, 1427 (2004).
[11] L. Lukaszuk and B. Nicolescu, Lett. Nuovo Cimento **8**, 405 (1973).
[12] A. Breakstone, H. B. Crawley, G. M. Dallavalle, K. Doroba, D. Drijard, F. Fabbri, A. Firestone, H. G. Fischer, H. Frehse, W. Geist *et al.*, Phys. Rev. Lett. **54**, 2180 (1985).
[13] S. Erhan, A. M. Smith, L. Meritet, M. Reyrolle, F. Vazeille, R. Bonino, A. Castellina, M. Medinnis, P. E. Schlein, P. Sherwood *et al.*, Phys. Lett. **152B**, 131 (1985).
[14] R. Avila, P. Gauron, and B. Nicolescu, Eur. Phys. J. C **49**, 581 (2007).
[15] V. M. Abazov *et al.* (D0 Collaboration), Phys. Rev. D **86**, 012009 (2012).

[16] G. Antchev *et al.* (TOTEM Collaboration), Eur. Phys. J. C **79**, 785 (2019).
[17] V. M. Abazov *et al.* (D0 and TOTEM Collaborations), Phys. Rev. Lett. **127**, 062003 (2021).
[18] J. Kwiecinski and M. Praszalowicz, Phys. Lett. **94B**, 413 (1980).
[19] J. Bartels, L. N. Lipatov, and G. P. Vacca, Phys. Lett. B **477**, 178 (2000).
[20] R. A. Janik and J. Wosiek, Phys. Rev. Lett. **82**, 1092 (1999).
[21] M. A. Braun, P. Gauron, and B. Nicolescu, Nucl. Phys. **B542**, 329 (1999).
[22] P. Gauron, L. N. Lipatov, and B. Nicolescu, Z. Phys. C **63**, 253 (1994).
[23] C. Ewerz, arXiv:hep-ph/0403051.
[24] J. Bartels, M. A. Braun, D. Colferai, and G. P. Vacca, Eur. Phys. J. C **20**, 323 (2001).
[25] E. R. Berger, A. Donnachie, H. G. Dosch, and O. Nachtmann, Eur. Phys. J. C **14**, 673 (2000).
[26] C. Adloff *et al.* (H1 Collaboration), Phys. Lett. B **544**, 35 (2002).
[27] L. A. Harland-Lang, V. A. Khoze, A. D. Martin, and M. G. Ryskin, Phys. Rev. D **99**, 034011 (2019).
[28] J. Czyzewski, J. Kwiecinski, L. Motyka, and M. Sadzikowski, Phys. Lett. B **398**, 400 (1997); **411**, 402(E) (1997).
[29] J. Bartels, M. A. Braun, and G. P. Vacca, Eur. Phys. J. C **33**, 511 (2004).
[30] G. P. Vacca, arXiv:hep-ph/0111174.
[31] R. Engel, D. Y. Ivanov, R. Kirschner, and L. Szymanowski, Eur. Phys. J. C **4**, 93 (1998).
[32] V. P. Goncalves and W. K. Sauter, Phys. Rev. D **91**, 094014 (2015).
[33] W. Kilian and O. Nachtmann, Eur. Phys. J. C **5**, 317 (1998).
[34] E. R. Berger and O. Nachtmann, Nucl. Phys. B, Proc. Suppl. **79**, 352 (1999).
[35] G. T. Bodwin, E. Braaten, and G. P. Lepage, Phys. Rev. D **51**, 1125 (1995); **55**, 5853(E) (1997).
[36] S. J. Brodsky and G. R. Farrar, Phys. Rev. Lett. **31**, 1153 (1973).
[37] G. P. Lepage and S. J. Brodsky, Phys. Rev. Lett. **43**, 545 (1979); **43**, 1625(E) (1979).
[38] A. V. Belitsky, X. d. Ji, and F. Yuan, Phys. Rev. Lett. **91**, 092003 (2003).
[39] Z. Ye, J. Arrington, R. J. Hill, and G. Lee, Phys. Lett. B **777**, 8 (2018).
[40] F. Feng, Y. Jia, and W. L. Sang, Phys. Rev. Lett. **115**, 222001 (2015).
[41] P. A. Zyla *et al.* (Particle Data Group), Prog. Theor. Exp. Phys. **2020**, 083C01 (2020).
[42] Y. Guo, X. Ji, and Y. Liu, Phys. Rev. D **103**, 096010 (2021).
[43] J. P. Ma, Nucl. Phys. **A727**, 333 (2003).
[44] E. J. Eichten and C. Quigg, arXiv:1904.11542.
[45] C. F. von Weizsacker, Z. Phys. **88**, 612 (1934).
[46] E. J. Williams, Kong. Dan. Vid. Sel. Mat. Fys. Med. **13N4**, 1 (1935), https://gymarkiv.sdu.dk/MFM/kdvs/mfm%2010-19/mfm-13-4.pdf.
[47] V. M. Budnev, I. F. Ginzburg, G. V. Meledin, and V. G. Serbo, Phys. Rep. **15**, 181 (1975).
[48] D. Kharzeev, H. Satz, A. Syamtomov, and G. Zinovjev, Eur. Phys. J. C **9**, 459 (1999).
[49] P. E. Shanahan and W. Detmold, Phys. Rev. D **99**, 014511 (2019).
[50] K. Azizi and U. Özdem, Eur. Phys. J. C **80**, 104 (2020).